UNSTEADY HARTMANN TWO-PHASE FLOW: THE SEMI-ANALYTICAL APPROACH

Sani Isa.* and Basant K. Jha.
*Author for correspondence
Department of Mathematics,
Ahmadu Bello University Zaria,
P. M. B. 1045, Samaru Zaria, Nigeria.
E-mail: sanimath@yahoo.com

ABSTRACT

Unsteady Hartmann two phase flows inside a parallel plate channel is considered due to sudden change in the applied pressure gradient. One of the fluids is assumed to be electrically conducting while the other fluid and the channel surfaces are assumed to be electrically non-conducting. The flow formation of conducting and non-conducting fluids is coupled by equating the velocity and shear stress at the interface. Both phases are incompressible and the flow is assumed to be fully-developed one- dimensional time dependent due to sudden change in applied pressure gradient. The relevant partial differential equations capturing the present physical situation are transformed in to ordinary differential equations using the Laplace transform technique. The ordinary differential equations are then solved exactly in the Laplace domain under relevant initial, boundary and interface conditions. The Riemann-sum approximation method is used to invert the Laplace domain into time domain. The solution obtained is validated by assenting comparisons with the closed form solutions obtained for steady states which has been derived separately and also by the implicit finite difference method. Variation of time-dependent velocity, mass flow rate and skin-friction (on channel surfaces) for various physical parameters involved in the problem are reported and discussed with the help of line graphs. There is an excellent agreement between time dependent solution and steady state solution at large value of time. Also velocity and mass flow rate decreases with increase of Hartmann number while it increases with increase in time.

INTRODUCTION

Studies in two-phase flows which are generally driven by gravitational and viscous forces results in the development of several multiphase theories arising in many engineering and scientific discipline that include petroleum industries, MHD devices, MHD power generator and magneto-fluid dynamics. There has been some theoretical and experimental work on stratified laminar flow of two immiscible fluids in a horizontal pipe. The interest in these types of problems stems from the possibility of reducing the power required to pump oil in pipe lines by suitable addition of water [1]. Shail [1] studied the steady Hartmann flow of a conducting fluid in a channel between two horizontal insulating parallel plates of infinite extent with a layer of non-conducting fluid between the upper wall and the conducting fluid. He observed that, an increase of order 30 % could be achieved in the flow rate for suitable ratios of heights and viscosities of the two fluids. Hartmann flow past a permeable bed in the presence of a transverse magnetic field with an interface at the surface of the permeable bed was presented by Rudraiah et al. [2]. Steady MHD channel flow has been enunciated in the pioneering work of Hartmann [3, 4]. Realizing the physical importance of these effects, Malashetty and Leela [5] and Lohrasbi and Sahai [6] studied the two-phase MHD flow and heat transfer in a parallel plate channel, where both phases are incompressible and the flow was assumed to be steady, one-dimensional and fully developed. These studies were an attempt to provide a clear understanding of the effect of slag layers on the heat transfer characteristics of a coal-fired MHD generator.

All the above studies dealt with the steady flow situations. However, there are many problems of practical interest that deals with two-fluid flow which are unsteady. In view of this, Umavathi *et al*. [7, 8] presented analytical solutions of unsteady/oscillatory Hartmann two-fluid and heat transfer in a horizontal channel. Unsteady MHD flow of two-fluid flow with time-dependent oscillatory wall transpiration velocity through a horizontal channel was investigated by Umavathi *et al* [9]. Raju

NOMENCLATURE

M	[-]	Hartmann number
P	[m^2K/W]	Pressure gradient
h	[m]	Channel height
x	[m]	Cartesian axis direction
y	[m]	Cartesian axis direction
z	[m]	Cartesian axis direction

Special characters

α	[-]	Ratio of densities of the two fluids
δ	[-]	Ratio of kinematic viscosities of the two fluids
ρ	[LM^3]	Density
μ	[-]	Kinematic viscosity
σ	[-]	electrical conductivity

Subscripts

1	lower phase
2	upper phase
I	interface

and Nagavalli [10] investigated the unsteady magnetohydrodynamic (MHD) two-layered fluids flow and heat transfer in a horizontal channel between two parallel plates in the presence of an applied magnetic and electric field, when the whole system is rotated about an axis perpendicular to the flow. Therefore, the aim of the present work is to present a semi-analytical solution of unsteady Hartmann two-phase flow between two parallel plates. Both phases are incompressible and the flow is assumed to be fully-developed and one-dimensional time dependent. One of the fluids is assumed to be electrically non-conducting.

MATHEMATICAL FORMULATION

The physical model shown in Figure 1 consists of two infinite parallel plates extending in the x - and z - direction. The region $0 \le y' \le d'$ is occupied by a fluid of viscosity μ_1 and electrical conductivity σ, and the region $d' \le y' \le h$ is occupied by a layer of non-conducting fluid of viscosity μ_2. A constant magnetic field of strength B_0 is applied in the y'-direction. The time dependent flow formation in both regions is due to sudden application of common pressure gradient $(-\frac{\partial p'}{\partial x'})$. The flow is assumed to be time-dependent, fully developed and the fluid properties are constants. Under the above stated assumptions, the dimensional equations of motion, and the corresponding initial boundary and interface conditions for the two phases are;

$$\frac{\partial u_1'}{\partial t'} = \upsilon_1 \frac{\partial^2 u_1'}{\partial y'^2} - \frac{\partial p'}{\partial x'}\frac{1}{\rho_1} - \frac{\sigma B_0^2}{\rho_1} u_1' \quad (1)$$

$$\frac{\partial u_2'}{\partial t'} = \upsilon_2 \frac{\partial^2 u_2'}{\partial y'^2} - \frac{\partial p'}{\partial x'}\frac{1}{\rho_1} \quad (2)$$

$$t' \le 0:\ u_1' = u_2' \ \text{ for } \ 0 \le y' \le h$$

$$t' > 0: \begin{cases} u_1'(0) = 0 \\ u_2'(h) = 0 \end{cases}$$

and

$$t' > 0 \ \text{ at } \ y' = d': \begin{cases} \mu_1 \frac{\partial u_1'}{\partial y'} = \mu_2 \frac{\partial u_2'}{\partial y'} \\ u_1' = u_2' \end{cases} \quad (3)$$

It is convenient to non-dimensionalise the above equations by using the following dimensionless quantities;

$$Y = \frac{y'}{h},\ (U_1; U_2) = (u_1'; u_2')\left(\frac{h}{\upsilon_1}\right), T = \frac{t'\upsilon_1}{h^2},\ M^2 = \frac{\sigma B_0^2 h^2}{\rho_1 \upsilon_1},$$
$$d = \frac{d'}{h},\ \alpha = \frac{\rho_1}{\rho_2}, \delta = \frac{\upsilon_2}{\upsilon_1},\ P = \frac{\partial p'}{\partial x'}\frac{1}{\rho_1}\frac{h^3}{\upsilon_1'} \quad (4)$$

where the subscripts 1 and 2 refer to the lower and upper phases, respectively. d is the dimensionless interface distance from the lower plate. α, δ are the ratios of densities and kinematics viscosities of the two fluids, T is the dimensionless time and M is the Hartman number, which is a measure of the strength of the applied magnetic field. Therefore, equations (1) - (3) respectively become,

$$\frac{\partial U_1}{\partial T} = \frac{\partial^2 U_1}{\partial Y^2} + P - M^2 U_1 \quad \text{for} \quad 0 \le Y \le d \quad (5)$$

$$\frac{\partial U_2}{\partial T} = \delta \frac{\partial^2 U_2}{\partial Y^2} + \alpha P \quad \text{for} \quad d \le Y \le 1 \quad (6)$$

$$T \le 0:\ U_1 = U_2 \text{ for } 0 \le Y \le 1$$

$$T > 0: \begin{cases} U_1(0) = 0 \\ U_2(1) = 0 \end{cases}$$

Subject to the following dimensionless initial, boundary and interface conditions:

$$T > 0 \ \text{ at } \ Y = d: \begin{cases} \frac{\partial U_1}{\partial Y} = \frac{\delta}{\alpha}\frac{\partial U_2}{\partial Y'} \\ U_1 = U_2 = U_I \end{cases} \quad (7)$$

Where U_I is the dimensionless interface velocity. Taking the Laplace transform of Equations (5) and (6) together with (7), we obtain the following ordinary differential equations, initial boundary and interface conditions;

$$\frac{d^2\overline{U}_1}{dY^2} - (M^2 + s)\overline{U}_1 = -\frac{P}{s} \quad (8)$$

$$\frac{d^2\overline{U}_2}{dY^2} - \frac{s}{\delta}\overline{U}_2 = -\frac{\alpha}{\delta}\frac{P}{s} \quad (9)$$

$$\overline{U}_1 = \overline{U}_2 \text{ for } 0 \le Y \le 1$$

$$\begin{cases} U_1(0) = 0 \\ U_2(1) = 0 \end{cases}$$

and

$$Y = d: \begin{cases} \frac{d\overline{U}_1}{dY} = \frac{\delta}{\alpha}\frac{d\overline{U}_2}{dY} \\ \overline{U}_1 = \overline{U}_2 = U_I s^{-1} \end{cases} \quad (10)$$

Where $\overline{U}_1 = \int_0^\infty U_1(Y,T)e^{-sT}dT$, $\overline{U}_2 = \int_0^\infty U_2(Y,T)e^{-sT}dT$ and $s > 0$ is the Laplace parameter. The solution of Equations (8) and (9) considering (10) are obtained respectively for $\overline{U}_1$ and $\overline{U}_2$ as follows;

$$\overline{U}_1 = \frac{U_I}{s}\frac{\sinh(\gamma Y)}{\sinh(\gamma d)} - \frac{P}{s\gamma^2}\left[\frac{\sinh(\gamma(d-Y))}{\sinh(d\gamma)} - 1\right] \quad (11)$$

$$\overline{U}_2 = \frac{\sinh(A(Y-1))}{\sinh(A(d-1))}\left[\frac{U_I}{s} + \frac{P}{s^2}\left\{\frac{\cosh dA}{\cosh(A)} - 1\right\}\right] + \frac{P\alpha}{s^2}\left[1 - \frac{\cosh(AY)}{\cosh(A)}\right] \quad (12)$$

and the interface velocity is obtained as

$$U_I = B\frac{P}{s}\left[\frac{\sinh(dA)}{\cosh(dA)} - \frac{\cosh(B(d-1))}{\sinh(B(d-1))}\left\{\frac{\cosh(dA)}{\cosh(A)} - 1\right\}\right] + A\left[\frac{P}{sA^2}\frac{1}{\sinh(d\gamma)} - \frac{p}{sA^2}\frac{\cosh(d\gamma)}{\sinh(d\gamma)}\right] \quad (13)$$

where $\gamma = \sqrt{M^2 + s}$, $A = \sqrt{\frac{s}{\delta}}$, $B = \sqrt{\frac{\delta}{s}}$

Equations (11) - (13) are to be inverted in terms of Riemann - sum approximation [11] as;

$$U(Y,T) = \frac{\exp(\epsilon T)}{T}\left[\frac{1}{2}\overline{U}(Y,\epsilon) + Re\sum_{k=1}^{N}\overline{U}\left(Y, \epsilon + \frac{ik\pi}{T}\right)(-1)^k\right] \quad (14)$$

where Re refers to the 'real part of', $i = \sqrt{-1}$ is imaginary number, N is the number of terms used in the Riemann-sum approximation and ϵ is the real part of the Bromwich contour that is used in inverting Laplace transforms. The Riemann-sum approximation for the Laplace inversion involves a single summation for the numerical process. Its accuracy depends on the value of ϵ and the truncation error dictated by N. According to Tzou [12], the value of ϵ must be selected so that the Bromwich contour encloses all the branch point. For faster

convergence the quantity $\epsilon T = 4.7$ gives the most satisfactory results since other tested values of ϵT seem to need longer computational time.

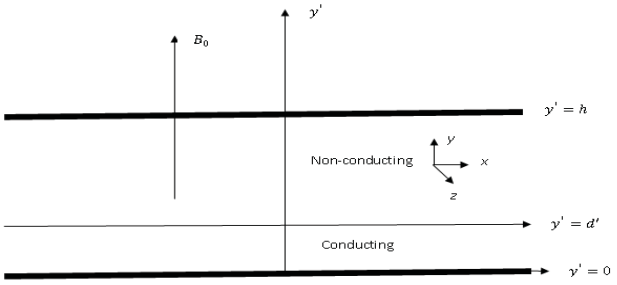

Figure 1 Physical configuration

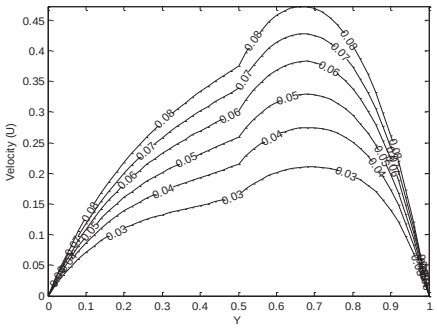

Figure 2 Profile of the velocity (U) showing the effect of time (T) for $M = 2,\ \alpha = 1.5,\ \delta = 0.5\ \ d = 0.5$ and $P = 5$

Skin-friction and Mass Flux

The skin friction τ_0 at the lower channel wall $(Y = 0)$ and τ_1 at the upper channel wall $(Y = 1)$ in terms of Laplace parameter s is computed by differentiating equations (11) and (12) respectively. Similarly, the mass flux in terms of the Laplace parameter s, $Q(Y, s)$ is obtained by adding the integrals of Eqs.(11) and (12). The expressions are given by:

$$\left.\frac{d\overline{U}_1}{dY}\right|_{Y=0} = c_2 A \qquad (15)$$

$$\left.\frac{d\overline{U}_2}{dY}\right|_{Y=1} = A[c_3 \sinh(B) + c_4 \cosh(B)] \qquad (16)$$

$$Q = \int_0^d \overline{U}_1(Y,s)dY + \int_d^1 \overline{U}_2(Y,s)dY$$
$$= \frac{1}{\gamma}[c_1 \sinh(d\gamma) + c_2\{\cosh(d\gamma) - 1\}]$$
$$+ B[c_3 \sinh(A) + c_4\{\cosh(A) - \cosh(Ad)\}]$$
$$+ \frac{Pd}{s\gamma^2} + \frac{P\alpha}{s^2}(1-d)$$

These given expressions are then converted to time domain by applying the Riemann-sum approximation stated in Eq.(14). Where

$$c_1 = -\frac{P}{s\gamma^2},\ c_2 = \left[\frac{U_I}{s} - \frac{P}{s\gamma^2}\right]\frac{1}{\sinh(\gamma d)} + \frac{P}{s\gamma^2}\frac{\cosh(\gamma d)}{\sinh(\gamma d)},\ ,$$
$$c_3 = \left[\frac{U_I}{s} + \frac{P\alpha}{s^2}\{\frac{\cosh(Ad)}{\sinh(A)} - 1\}\right]\frac{\sinh(A)}{\sinh(A(d-1))} - \frac{P\alpha}{s^2\cosh(A)},$$
$$c_4 = \left[\frac{U_I}{s} + \frac{P\alpha}{s^2}\{\frac{\cosh(Ad)}{\sinh(A)} - 1\}\right]\frac{\cosh(A)}{\sinh(A(d-1))}$$

Validation of Method

In order to validate the accuracy of the Riemann-sum approximation method, we set out to find the solution of the steady state, which should coincide with the transient solution at large time. The equations for the steady state velocities (U_{s1}, U_{s2}) for the two phases are obtained by setting $\frac{\partial()}{\partial T}$ in Equations (5) and (6) to zero. Then the following equations results

$$\frac{d^2U_{s1}}{dY^2} - M^2U_{s1} = -P \qquad (18)$$

$$\frac{d^2U_{s2}}{dY^2} = -\frac{\alpha P}{\gamma} \qquad (19)$$

The boundary and interface conditions are

$$U_{s1}(0) = 0;\ \ U_{s1}(1) = 0.$$

$$Y = d: \begin{cases} \frac{dU_{s1}}{dY} = \frac{\delta}{\alpha}\frac{dU_{s2}}{dY} \\ U_{s1} = U_{s2} \end{cases} \qquad (20)$$

The solution of equations (18) and (19) considering (20) which is the steady state velocities for the two phases U_{s1} and U_{s2} are given as;

$$U_{s1}(Y) = \frac{U_{sI}\sinh(MY)}{\sinh(Md)} + \frac{P}{M^2} - \frac{P}{M^2}\frac{\sinh(M(d-Y))}{\sinh(Md)} - \frac{P}{M^2}\frac{\sinh(MY)}{\sinh(Md)} \qquad (21)$$

$$U_{s2}(Y) = \frac{U_{s1}(Y-1)}{(d-1)} + \frac{P\alpha}{2\gamma}\{(Y-1)d + (Y-Y^2)\} \qquad (22)$$

The steady state skin-friction (τ_s) is obtained by differentiating equations (21) and (22) with respect to Y. then, the steady state skin-friction on the lower (τ_0) and upper (τ_1) plates are then computed by setting $Y = 0$ and $Y = 1$ as;

$$\left.\frac{dU_{s1}}{dY}\right|_{Y=0} = \frac{P[\cosh(Md)-1]}{M\sinh(Md)} + \frac{MU_{s1}}{\sinh(Md)},\ \left.\frac{dU_{s2}}{dY}\right|_{Y=1} = \frac{U_{sI}}{(d-1)}$$

And the steady state mass flux is given as;

$$Q_s = \int_0^d U_{s1}(Y)dY + \int_d^1 U_{s2}(Y)dY = \frac{U_{sI}[\cosh(Md)-1]}{M\sinh(Md)} +$$
$$\frac{U_{sI}\left[\frac{1-d^2}{2} - (1-d)\right]}{(d-1)} + \frac{P\alpha\left[d\{\frac{1-d^2}{2} - (1-d)\}\right]}{2\gamma} + \frac{P\alpha\left[d\{\frac{1-d^2}{2} - (\frac{1-d}{3})\}\right]}{2\gamma} -$$
$$\frac{P}{M^2}\left[\frac{2(\cosh(Md)-1)}{M\sinh(Md)} - d\right] \qquad (23)$$

Where

$$U_{sI} = \frac{1}{F}\left[\frac{1}{2}(1-d) - \frac{P}{M}\left(\frac{1}{\sinh(Md)} - \frac{\cosh(Md)}{\sinh(Md)}\right)\right]$$

$$F = \frac{M\cosh(Md)}{\sinh(Md)} - \frac{\gamma}{\alpha}\frac{1}{d-1}$$

Finite Difference Method

In this section, implicit finite difference method is used to ascertain the correctness of the Riemann-sum approximation method. The procedure we have adopted involves dividing the solutions into grid points and approximating the differential equations by the finite difference equations and then solving the difference equations subject to the prescribed initial, boundary and interface conditions. Thus eqns.(5) and (6) become

$$\frac{U_1(i,j) - U_1(i,j-1)}{\Delta T} = \frac{U_1(i+1,j) - 2U_1(i,j) + U_1(i-1,j)}{\Delta Y^2} + P - M^2U_1(i,j) \qquad (24)$$

$$\frac{U_2(i,j) - U_2(i,j-1)}{\Delta T} = \frac{\delta U_2(i+1,j) - 2U_2(i,j) + U_2(i-1,j)}{\Delta Y^2} + P\alpha \qquad (25)$$

The index i refers to Y and j refers to T. The time derivative is replaced by the backward difference formula, while the spatial derivatives are replaced by central difference formula. The above equations are solved by Thomas algorithm by manipulating into a system of linear algebraic equations in the tridiagonal form. At each time step, the process of numerical integration for every dependent variable starts from the first neighbouring grid point of the lower plate at $Y = 0$ and proceeds towards the upper plate at $Y = 1$. The process of computation is advanced until a steady state is approached by satisfying the following convergence criterion:

$$\frac{\sum|A_{i,j+1}-A_j|}{M^*|A|_{max}} \leq 10^{-6} \quad (26)$$

with respect to the fluids velocity. Here $A_{(i,j)}$ stand for the velocity field. M^* is the number of interior grid points and $|A|_{max}$ is the maximum absolute value of $A_{(i,j)}$. In the numerical computation special attention is needed to specify ΔT to get steady state solution as rapid as possible, yet small enough to avoid instabilities. It is set, which is suitable for the present computation, as

$$\Delta T = Stabr \times (\Delta Y)^2 \quad (27)$$

The parameter $Stabr$ is determined by numerical experimentation in order to achieve convergence and stability of the solution procedure. Numerical experiments show that the value 2 is suitable for the present numerical computation.

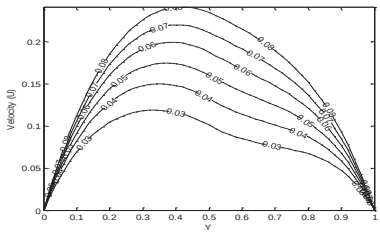

Figure 3 Profile of the velocity (U) showing the effect of time (T) for $M = 2, \alpha = 0.5,\ \delta = 0.5, d = 0.5$ and $P = 5$

RESULTS AND DISCUSSION

In order to get a physical insight into the problem, the velocity, the interface velocity, the skin-friction and the mass flux are presented graphically for different values dimensionless time (T), the Hartmann number (M), ratios of densities of the two fluids (α), ratios of kinematic viscosities of the two fluids (δ) and pressure gradient (P). Both fluids are considered to have different densities, viscosities, one is electrically conducting while the other is electrically non-conducting, and occupy equal heights (d=0.5). To authenticate the semi-analytical solution obtained by the Riemann-sum approximation method, separate closed form solutions were obtained for steady state and also by implicit finite difference method taking into account suitable interface matching conditions. A good agreement was found between the obtained results as time progress as seen in table 1. Figures 2 and 3 demonstrate the effect of time (T) on the velocity profiles for fixed values of $M = 2, d = 0.5$ and $P = 5$. It is observed that an increase in T increases the velocity in both phases and finally attains steady state. Furthermore, when the ratio of density is less than unity $(\alpha = 0.5)$ maximum velocity occurs in conducting fluid $(0 \leq Y \leq 0.5)$ while the result is just reverse when the density ratio is greater than unity $(\alpha = 1.5)$. This is due to the fact that when the ratio of density is less than unity, conducting fluid density is lower than the density of non-conducting fluid. Hence, common application of pressure gradient is more effective in fluid layer having low density. Fig. 4 depicts the influence of Hartmann number (M) on the velocity. It is clear that as M increases the velocity decreases in conducting as well as non-conducting fluid. The decrease in the non-conducting fluid is due to the interface condition. Also the role of Hartmann number is dominant in conducting fluid. Fig.5 reveals the role of pressure gradient on velocity. By definition positive pressure gradient (i.e pressure decreases along the flow direction). The negative rate of pressure (P) represent adverse pressure gradient (i.e pressure increases along flow direction). From this Figure, it is observed that an increase in positive value of P accelerate the velocity while negative value of P accelerate the reverse flow. Fig.6 depicts the variation of ratio of viscosity (δ) on velocity. It is clear that as δ increases velocity increases in both fluids. The effect of density ratio on velocity field is shown in Fig.7. it is found that an increase in α increases the velocity. It is also interesting to note that the impact of α is dominant in non-conducting layer. The variation of interface velocity (U_I) is depicted in Fig.8 with respect to time and Hartmann number. It is observed that interface velocity decreases with Hartmann number while it increases with time. The role of interface distance (d) and time on interface velocity is displayed in Fig. 9. It is evident that as d increases interface velocity decreases while it increases with time. The effect of ratio of viscosity and time on the interface velocity is shown in Fig.10. it is observed that interface velocity increases with time and finally attains steady state value while it decreases with δ. The influence of density ratio (α) and time on interface velocity is shown in Fig.11. This Figure reveals that interface velocity increase with α and time. In Fig.12, the skin-friction (τ_0) at $Y = 0$ is shown with respect to time and Hartmann number. This Figure shows that as Hartmann number increases, skin-friction decreases with time. Skin-friction variation at the lower plate with time and pressure gradient is displayed in Fig.13. it reveals that skin-friction is higher for negative value of P. Also it increases with time for negative value of P while it decreases for positive value of P with increment of time. Fig.14 shows the effect of Hartmann number and time on skin-friction at $Y = 1$. An increase in Hartmann number decreases the skin-friction while it increases with time. Fig.15 shows the role of pressure gradient and time on skin-friction at $Y = 1$. It is observed that the result is just reverse as observed at $Y = 0$ (see Fig. 13). The dimensionless mass flux variation with Hartmann number and time is displayed in Fig.16. From this Figure it is clear that mass flux decreases with Hartmann number while it increases with time. The effect of time as well as pressure gradient on mass flux is shown in Fig.17. it is evident that mass flux increases with positive value of P and time while the result is just reverse for negative value of P.

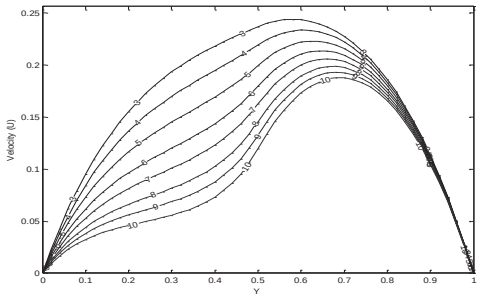

Figure 4 Profile of the velocity (U) showing the effect of M for $T = 0.06$, $\alpha = 1$, $\delta = 1$, $d = 0.5$ and $P = 5$

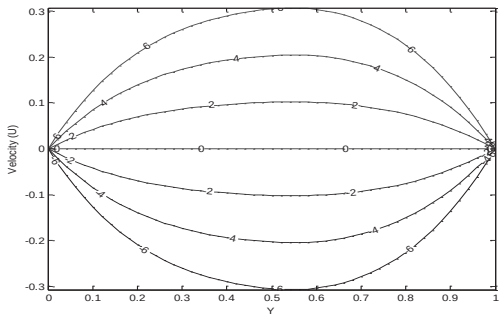

Figure 5 Profile of the velocity (U) showing the effect of P for $T = 0.06$, $\alpha = 1$, $\delta = 1$, $d = 0.5$ and $M = 2$.

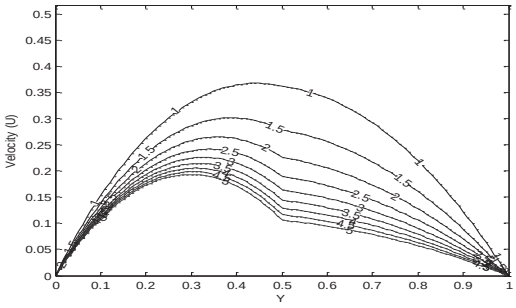

Figure 6 Profile of the velocity (U) showing the effect of ratio of fluids viscosity (δ) for $M = 2$, $\alpha = 0.5$, $d = 0.5$, $T = 0.6$ and $P = 5$.

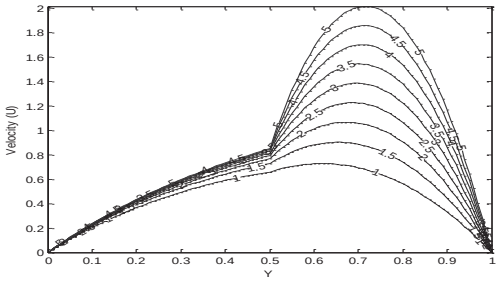

Figure 7 Profile of the velocity (U) showing the effect of ratio of fluids density (α) for $M = 2$, $\delta = 0.5$ $d = 0.5$, $T = 0.6$ and $P = 5$.

Conclusion

In this paper, we have studied the problem of time-dependent Hartmann two-phase flow between two parallel plates of infinite extent, consisting of two regions one electrically conducting and the other electrically non-conducting. Semi-analytical solutions are obtained using the combination of Laplace transform technique and the Riemann-sum approximation method and the following conclusions are drawn;

1. Flow formation is strongly dependent on nature of the fluids trapped inside the channels
2. Increase in M decreases the velocity (U) and mass flux (Q)
3. Interface velocity decreases as M, δ and d increases
4. Skin-frictions and mass flux increases with time and favourable pressure gradient.

REFERENCES

[1] Shail R., On Laminar Two-Phase Flows in Magnetohydrodynamics, *International Journal of Engineering Science*, Vol.11, 1973, pp. 1103-1108

[2] Rudraiah, N, Ramaih, B. K., and Rajashekhar, B. M. Hartmann flow over a permeable bed, *International Journal of Engineering Science*, Vol. 13, 1975, pp. 1-24

[3] Hartmann, J. and Lazarus, F., Experimental investigations on the flow of Mercury in a homogeneous magnetic field, *Det Kgl . Danske Videnskabernes Selskab. Mathematisk-fysiske Meddelelser*, Vol XV7, 1937

[4] Hartmann, J., theory of Laminar flow of an electrically conducting liquid in a homogeneous magnetic field, *Det Kgl . Danske Videnskabernes Selskab. Mathematisk-fysiske Meddelelser* Vol .XV 6, 1937.

[5] Malashetty, M. S. and Leela, V., Magnetohydrodynamic Heat Transfer in two phase flow, International. Journal of Engineerinng. Science ,Vol.30, 1, 1992, pp 371 - 377.

[6].Lohrasbi, J. and Sahai, V., Magnetohydrodynamic heat transfer in two-phase flow between parallel plates, *Applied Scientific, Research*, Vol. 45, 1988, pp 53 – 66.

[7] Umavathi, J. C., Chamkha, A. J., Mateen, A. and Al-Mudhaf, A., Unsteady two-fluid flow and heat transfer in a horizontal channel, *Heat and Mass Transfer*, Vol.42,2, 2005, pp81 - 90.

[8] Umavathi, J. C., Mateen,, A. , Chamkha, A. J. , and Al-Mudhaf, A., Oscillatory Hartmann two-fluid flow and heat transfer in a horizontal channel, *International Journal of Applied Mechanics and Engineering*, Vol.11,1, 2006, pp155 – 178.

[9] Umavathi, J. C., Chamkha, A. J., Mateen, A. and Kumar, J. P., Unsteady magnetohydrodynamic two-fluid flow and heat transfer in a horizontal channel, *Heat and Technology*, Vol.26,2, 2008, pp 121 - 133.

[10] Raju Linga, T. and Nagavalli, M., MHD Two -Layered unsteady fluid flow and heat transfer through a horizontal channel between parallel plates in a rotating system, *International Journal of Applied Mechanics and Engineering*, Vol.19,1, 2014, pp 97 - 121.

[11] Jha, B.K. and Apere, C.A. Unsteady MHD Couette flow in an annuli: the Riemann-sum approximation approach, Journal of Physical Society of Japan, Vol.79, 2010, 124403

[12] Tzou, D.Y. Macro to Microscale Heat Transfer: The Lagging Behaviour, *Taylor and Francis*, 1997.

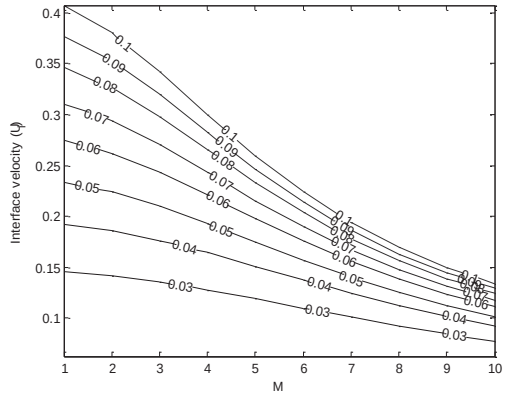

Figure 8 Interface velocity (U_i) against M showing the effect of time (T) for $\alpha = 1.0,\ \delta = 0.5\ d = 0.5$ and $P = 5$.

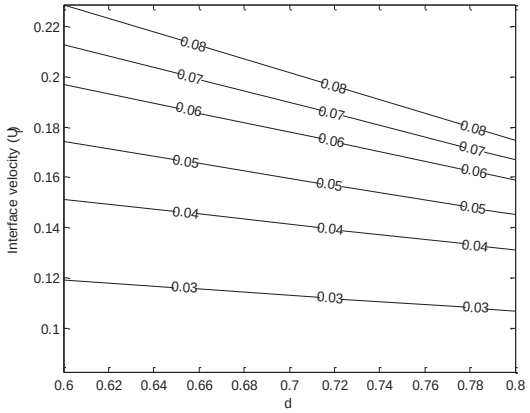

Figure 9 Interface velocity (U_i) against d showing the effect of time (T) for $\alpha = 1.0,\ \delta = 0.5\ M = 2$ and $P = 5$.

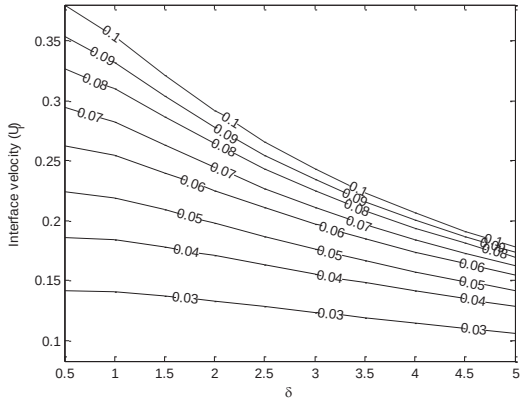

Figure 10 Interface velocity (U_i) against δ showing the effect of time (T) for $\alpha = 1.0,\ d = 0.5\ M = 2$ and $P = 5$.

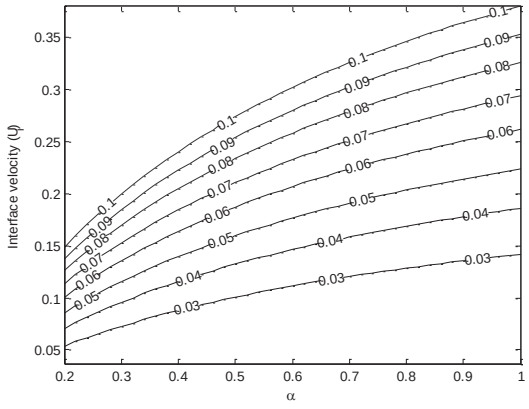

Figure 11 Interface velocity (U_i) against α showing the effect of time (T) for $\delta = 1.0,\ d = 0.5\ M = 2$ and $P = 5$.

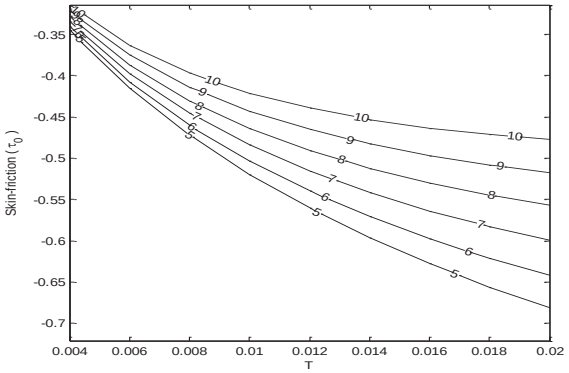

Figure 12 Variation of the Skin-friction (τ_0) on the plate at $Y = 0$ showing the effect of M and T for $\alpha = 1$, $\delta = 1,\ d = 0.5$ and $P = 5$.

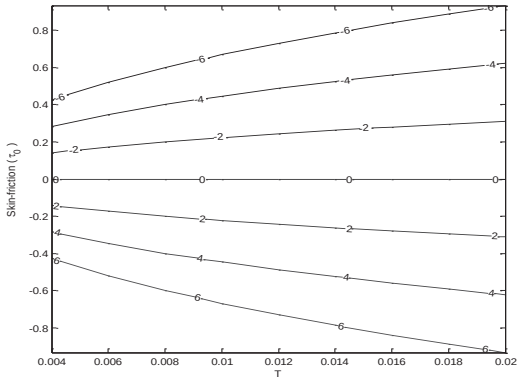

Figure 13 Variation of the Skin-friction (τ_0) on the plate at $Y = 0$ showing the effect of P and T for $\alpha = 1$, $\delta = 1,\ d = 0.5$ and $M = 2$.

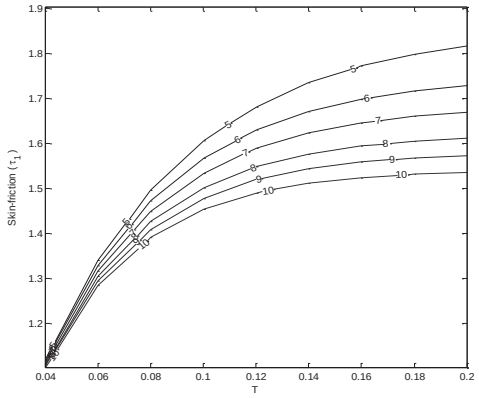

Figure 14 Variation of the Skin-friction (τ_1) on the plate at $Y = 1$ showing the effect of M and T for $\alpha = 1$, $\delta = 1$, $d = 0.5$ and $P = 5$.

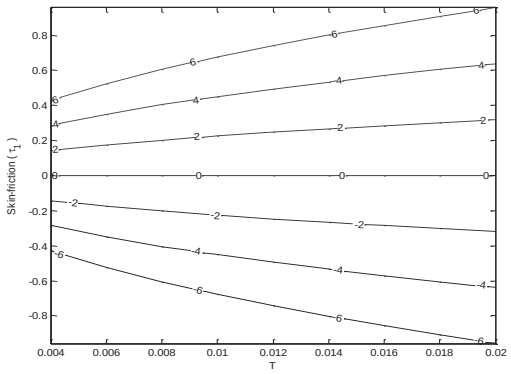

Figure 15 Variation of the Skin-friction (τ_1) on the plate at $Y = 1$ showing the effect of P and T for $\alpha = 1$, $\delta = 1$, $d = 0.5$ and $M = 2$.

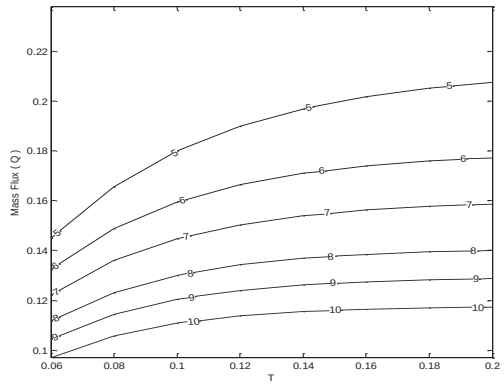

Figure 16 Dimensionless Mass Flux (Q) showing the influence of M and T for $\alpha = 1$, $\delta = 1$, $d = 0.5$ and $P = 5$.

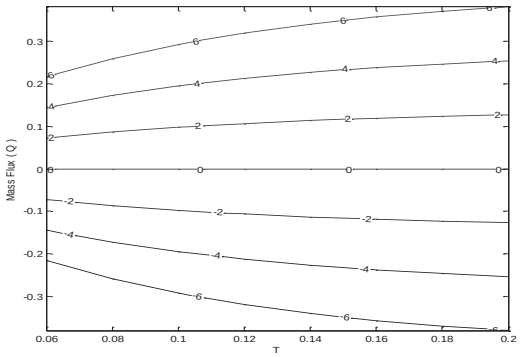

Figure 17 Dimensionless Mass Flux (Q) showing the influence of P and T for $\alpha = 1$, $\delta = 1$, $d = 0.5$ and $M = 2$.

Table:1 Comparison of the numerical values obtained using Riemann-sum approximation method (RSM) and that obtained using finite difference method (FDM) and the steady state when $M = 2.0, \delta = 1.0, \alpha = 1.0, d = 0.5$ and $P = 5.0$

T	Y	Velocity		
		Transient		Steady State
		RSM	FDM	
0.2	0.2	0.2902	0.2829	0.3177
	0.4	0.4375	0.4284	0.4841
	0.6	0.4653	0.4503	0.5160
	0.8	0.3252	0.3168	0.3580
0.4	0.2	0.4798	0.4766	0.3177
	0.4	0.4828	0.4815	0.4841
	0.6	0.5112	0.5078	0.5160
	0.8	0.3549	0.3529	0.3580
0.6	0.2	0.3175	0.3171	0.3177
	0.4	0.4838	0.4832	0.4841
	0.6	0.5156	0.5150	0.5160
	0.8	0.3577	0.3574	0.3580
0.7	0.2	0.3176	0.3175	0.3177
	0.4	0.4841	0.4838	0.4841
	0.6	0.5159	0.5156	0.5160
	0.8	0.3579	0.3578	0.3580
0.8	0.2	0.3177	0.3176	0.3177
	0.4	0.4841	0.4840	0.4841
	0.6	0.5160	0.5155	0.5160
	0.8	0.3580	0.3579	0.3580